

Zinc oxide and its anion: A negative ion photoelectron spectroscopic study

C. A. Fancher, H. L. de Clercq, O. C. Thomas, D. W. Robinson, and K. H. Bowen^{a)}

Department of Chemistry, Johns Hopkins University, Baltimore, Maryland 21218

(Received 18 May 1998; accepted 14 August 1998)

We have recorded, assigned, and analyzed the photoelectron spectrum of ZnO^- . The adiabatic electron affinity ($E.A._a$) of ZnO and the vibrational frequencies of both ZnO and ZnO^- were determined directly from the spectrum, with a Franck–Condon analysis of its vibrational profile providing additional refinements to these parameters along with structural information. As a result, we found that $E.A._a(\text{ZnO}) = 2.088 \pm 0.010$ eV, $\omega_e(\text{ZnO}) = 805 \pm 40$ cm^{-1} , $\omega_e(\text{ZnO}^-) = 625 \pm 40$ cm^{-1} , and that $r_e(\text{ZnO}^-) > r_e(\text{ZnO})$ by 0.07 Å. Since our measured value of $E.A._a(\text{ZnO})$ is 0.63 eV larger than the literature value of $E.A.(O)$, it was also evident, through a thermochemical cycle, that $D_0(\text{ZnO}^-) > D_0(\text{ZnO})$ by 0.63 eV. This, together with the literature value of $D_0(\text{ZnO})$, gives a value for $D_0(\text{ZnO}^-)$ of 2.24 eV. Since the extra electron in ZnO^- is expected to occupy an antibonding orbital, the combination of $D_0(\text{ZnO}^-) > D_0(\text{ZnO})$, $\omega_e(\text{ZnO}^-) < \omega_e(\text{ZnO})$, and $r_e(\text{ZnO}^-) > r_e(\text{ZnO})$ was initially puzzling. An explanation was provided by the calculations of Bauschlicher and Partridge, which are presented in the accompanying paper. Their work showed that our experimental findings can be understood in terms of the $a^3\Pi$ state of ZnO dissociating to its ground-state atoms, while the $X^1\Sigma^+$ state of ZnO formally dissociates to a higher energy atomic asymptote. © 1998 American Institute of Physics. [S0021-9606(98)01843-1]

INTRODUCTION

Bulk zinc oxide is a *n*-type, large band gap semiconductor, and it finds uses in pigments, catalysts, and topical medicines. While considerable empirical information^{1–3} is available about zinc oxide as a solid and even about zinc oxide nanoparticles, somewhat less is known about the properties of individual ZnO molecules, impeding progress in modeling the materials properties of zinc oxide. Nevertheless, several studies have been conducted on molecular zinc oxide over the years. Much of the experimental work has focused on the sublimation and thermodynamic properties of zinc oxide. In 1951, Brewer and Mastick⁴ found that zinc oxide sublimates by decomposition to its elements, and in 1953, Brewer⁵ estimated an upper limit of 3.9 eV for the heat of dissociation of ZnO. There followed several studies of the unusual sublimation behavior of zinc oxide.^{6–10} Then, in 1964, Anthrop and Searcy¹¹ utilized high-temperature mass spectrometry to set an upper limit of 2.86 eV for the dissociation energy of ZnO, $D_0(\text{ZnO})$, even though they did not actually observe the zinc oxide parent ion. Next, in 1983, Wicke¹² proposed a lower limit of 2.8 eV for $D_0(\text{ZnO})$ based on his $\text{Zn} + \text{N}_2\text{O}$ chemiluminescence measurements. Both prior and subsequent theoretical studies, however, all gave results for $D_0(\text{ZnO})$ which were well below this value.^{13–17} More recently, in 1991, the issue of the dissociation energy of ZnO was revisited by Armentrout and co-workers.¹⁸ Gas-phase thermochemical information, including $D_0(\text{ZnO})$, was extracted from guided ion beam mass spectrometric studies of the Zn^+ and NO_2 reaction. Their value of $D_0(\text{ZnO})$ was 1.61 ± 0.04 eV. Since then, Watson and co-workers,¹⁹ using high-temperature mass spectrometric techniques, have set an

upper limit of 2.3 eV for $D_0(\text{ZnO})$. In addition to the foregoing work, Prochaska and Andrews²⁰ also conducted matrix isolation studies of ZnO in nitrogen, determining the vibrational frequency for ZnO in the matrix environment (808.6 cm^{-1} , average value over Zn isotopes).

Here, we present results from our negative ion photoelectron spectroscopic study of ZnO^- . Much of the information provided by such experiments pertains not only to the anion, but also to its corresponding neutral at the geometry of the anion. Assignment of the vibronic features in the photoelectron spectrum led not only to the determination of the adiabatic electron affinity for ZnO, $E.A._a(\text{ZnO})$, but also to the vibrational frequencies of both ZnO and ZnO^- in the gas phase. The measured value of $E.A._a(\text{ZnO})$, together with literature values of $D_0(\text{ZnO})$ and $E.A.(O)$, led, through a thermochemical cycle, to $D_0(\text{ZnO}^-)$. A Franck–Condon analysis of the spectrum gave the change in bond length between ZnO and ZnO^- , as well as further refinements to the vibrational frequencies of ZnO and ZnO^- . In addition, complementary electronic structure calculations on ZnO and ZnO^- were conducted by Bauschlicher and Partridge,¹⁷ and their work, which played a key role in the interpretation of our results, is presented in the accompanying paper. Prior to this collaborative effort, neither experimental nor theoretical studies had been conducted on the zinc oxide anion, ZnO^- .

EXPERIMENT

Negative ion photoelectron spectroscopy is conducted by crossing a mass-selected beam of negative ions with a fixed-frequency photon beam and energy analyzing the resultant photodetached electrons. This is a direct approach for determining electron binding energies (EBE), relying as it does on the relationship

$$h\nu = \text{EBE} + KE_e, \quad (1)$$

^{a)} Author to whom correspondence should be addressed. Electronic mail: kitbowen@jhunix.hcf.jhu.edu

in which $h\nu$ is the photon energy, and KE_e is the measured electron kinetic energy. Our apparatus²¹ has been described in detail previously. The photoelectron spectrum of ZnO^- was calibrated against the well-known photoelectron spectra of K^- and O^- and was recorded at an electron energy analyzer resolution of 23 meV, using both the 488.0 nm (2.540 eV) and 457.9 nm (2.707 eV) lines of an argon ion laser. Switching the photon energy from one to the other caused no apparent change in the observed spectrum (electron intensity vs EBE).

Zinc oxide anions were generated in this experiment using a "pick-up" version of our hot, supersonic expansion ion source.²² Because bulk zinc oxide decomposes upon being heated to temperatures at which it vaporizes, thermal evaporation of solid ZnO samples is not a suitable method for getting ZnO molecules into the gas phase, and no doubt, this state of affairs has impeded the experimental study of molecular ZnO in the past. Our pick-up ion source circumvented this problem by preparing ZnO^- in the partially ionized gaseous environment just outside the nozzle of the source. This was accomplished by evaporating zinc metal in the stagnation chamber (oven) of the source at 650 °C, expanding it through a 125 μm dia nozzle orifice (@700 °C) with 200–300 Torr of argon, and adding (via an effusive flow) a small amount of N_2O to the region immediately outside the nozzle via a separate pick-up line. In this same region, anions were formed by injection of electrons from a thoriated iridium filament directly into the expanding jet in the presence of an axial magnetic field. Typically, the filament was biased at -75 V relative to the stagnation chamber, giving an emission current of ~ 10 mA. The stagnation chamber itself was floated at -500 V, i.e., the beam energy. Under these conditions, this ion source provided 20–30 pA of ZnO^- ion current in the ion-photon interaction region of the spectrometer.

RESULTS AND ANALYSIS

Because of its closed-shell electronic structure, zinc stands apart from the other first row transition metals. It bonds primarily through its $4s$ and $4p$ orbitals, leaving its $3d$ subshell largely unengaged and making it more analogous to the alkaline earth metals than to other transition metals. Thus, just as in the cases of MgO and CaO, ZnO is expected to have a $^1\Sigma^+$ ground state.^{14,17} The ground state of ZnO^- , on the other hand, is expected to be $^2\Sigma^+$, with its extra electron having gone into an antibonding orbital.¹⁷

The photoelectron spectrum of ZnO^- recorded with the 457.9 nm (2.707 eV) line of an argon ion laser is presented in Fig. 1. We attribute the observed vibronic profile primarily to $\text{ZnO}^-(X^2\Sigma^+;v'') \rightarrow \text{ZnO}(X^1\Sigma^+;v')$ transitions. The vibrational spacings observed toward the high EBE side of this profile compare well with the literature value²⁰ for the vibrational frequency of neutral ZnO, while the lone, distinct vibrational spacing observed on its low EBE side is somewhat smaller. Given that the vibrational frequency of ZnO^- is expected to be significantly less than that of ZnO, and that hot bands appear most prominently on the low EBE side of vibronic profiles, the assignment of this spectrum is straightforward (see Fig. 2). The EBE of the $(v''=0, v'=0)$ transi-

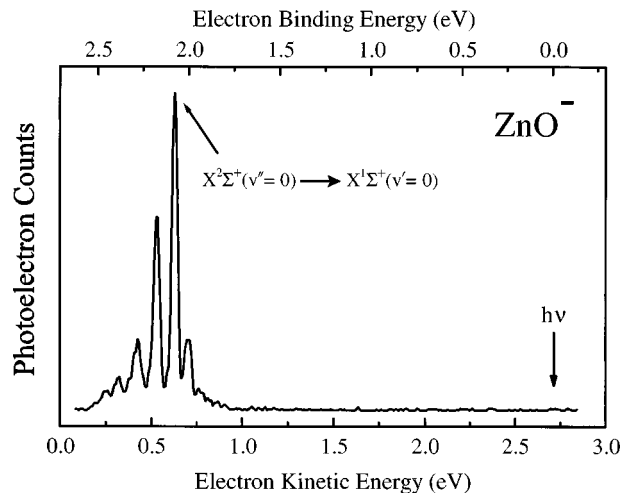


FIG. 1. The photoelectron spectrum of ZnO^- recorded with 2.707 eV photons.

tion (indicated in both Figs. 1 and 2) is equal to the value of the adiabatic electron affinity, and for ZnO, we have determined $E.A._a$ to be 2.088 eV.

The relationship between the $E.A._a(\text{ZnO})$, $E.A.(\text{O})$, $D_0(\text{ZnO})$, and $D_0(\text{ZnO}^-)$, where $D_0(\text{ZnO}^-)$ pertains to ZnO^- dissociating into $\text{Zn}(^1S) + \text{O}(^2P)$, is

$$E.A._a(\text{ZnO}) - E.A.(\text{O}) = D_0(\text{ZnO}^-) - D_0(\text{ZnO}). \quad (2)$$

Having determined $E.A._a(\text{ZnO})$ to be 2.088 eV and knowing the literature value²³ of $E.A.(\text{O})$ to be 1.46 eV, it is clear from our data alone that $D_0(\text{ZnO}^-) > D_0(\text{ZnO})$ by 0.63 eV. Armentrout's experimental value¹⁸ of 1.61 ± 0.04 eV for $D_0(\text{ZnO})$ is in excellent agreement with Bauschlicher and Partridge's very recent, high level computational value¹⁷ of 1.63 eV, further supporting the reliability of his measurement. Using 1.61 eV for $D_0(\text{ZnO})$ in Eq. (2), gives a value for $D_0(\text{ZnO}^-)$ of 2.24 eV. At first sight, our finding that $D_0(\text{ZnO}^-) > D_0(\text{ZnO})$ is surprising, since the excess elec-

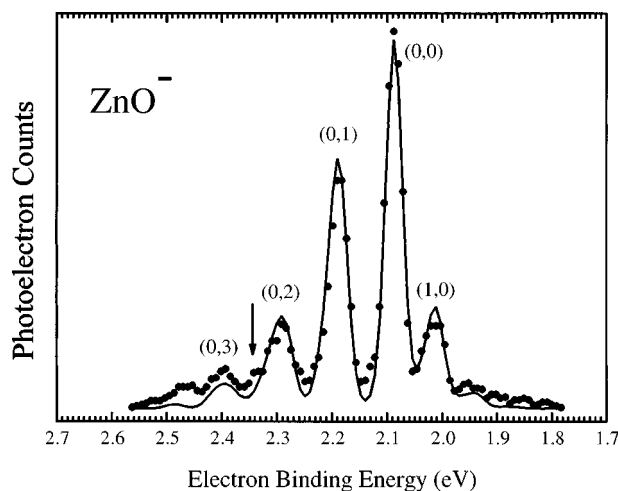


FIG. 2. The measured (dots) and the simulated (smooth trace) photoelectron spectra of ZnO^- . Spectral assignments are indicated as (v'',v') for the transitions, $\text{ZnO}^-(X^2\Sigma^+;v'') \rightarrow \text{ZnO}(X^1\Sigma^+;v')$. A vertical arrow marks the suspected origin of transitions from the $X^2\Sigma^+$ state of ZnO^- to the excited $a^3\Pi$ state of ZnO.

tron in ZnO^- is thought to reside in an antibonding orbital of ZnO . This dilemma is explained, however, both in the accompanying paper by Bauschlicher and Partridge¹⁷ and in the Discussion section below.

Franck–Condon analysis of the ZnO^- photoelectron spectrum corroborated our assignment of the spectrum and provided values for several molecular constants. This analysis was conducted using a program developed by Ervin and Lineberger.^{24,25} It models both anion and neutral electronic potential curves as Morse oscillators. Experimental determinations of the vibrational frequency of ZnO , $\omega_e(\text{ZnO})$, were available both from the peak spacings in our spectrum and from the matrix study by Andrews.²⁰ The spectral simulation was run using both numbers and was found to converge to the same value. The hot band vibrational spacing observed on the low EBE side of the spectrum served as initial input for the vibrational frequency of ZnO^- . Because there were no values available for $\omega_e x_e$, these were estimated for both the neutral and the anion from analogous molecules. Since ZnO should have similar bonding to the alkaline earth metal oxides, the anharmonicity of CaO (4.8 cm^{-1}) was used to estimate $\omega_e x_e$ in ZnO . The anharmonicity of GaO (6.24 cm^{-1}) was used to estimate $\omega_e x_e$ in ZnO^- , since GaO is isoelectronic with ZnO^- and close in mass. The intensity and spectral position of the (0,0) transition was measured directly from the photoelectron spectrum. During the simulation of the spectrum, the vibrational frequencies of the anion and neutral, the vibrational temperature, r_e of the anion, and the full-width-half-maximum of the peaks were allowed to vary. The best fit to the spectrum is shown in Fig. 2, along with our assignments. Refined (best fit) vibrational frequencies coming from this analysis were $\omega_e(\text{ZnO}) = 805 \pm 40 \text{ cm}^{-1}$ and $\omega_e(\text{ZnO}^-) = 625 \pm 40 \text{ cm}^{-1}$. This value for $\omega_e(\text{ZnO})$ is the first gas-phase determination of the vibrational frequency of ZnO . The vibrational temperature converged to $\sim 900 \text{ K}$, roughly the temperature of the stagnation chamber of the source. This analysis also provided the change in the bond length (r_e) of ZnO compared with ZnO^- , i.e., Δr_e . The Franck–Condon analysis of our spectrum alone found the ZnO^- bond to be 0.07 \AA longer than the bond in ZnO , i.e., $\Delta r_e = +0.07 \text{ \AA}$. Using the calculated value of $r_e(\text{ZnO})$ from the work of Bauschlicher and Partridge¹⁷ implies that $r_e(\text{ZnO}^-) = 1.79 \text{ \AA}$. The molecular constants derived from this analysis are summarized in Table I, along with their calculated values from the work of Bauschlicher and Partridge.¹⁷

Like the alkaline earth oxides, ZnO is expected to have a $^3\Pi$ first excited state. Unlike the alkaline earth oxides, however, the $^3\Pi$ state in ZnO is predicted to be quite low lying. Recent calculations by Bauschlicher and Partridge,¹⁷ presented in the companion paper, put the $^3\Pi$ state of ZnO just 0.26 eV above its $X^1\Sigma^+$ state. This implies that photodetachment transitions to the $^3\Pi$ state of ZnO should be observable within our experimental energy window, their origin starting at an EBE of 2.35 eV and extending to higher EBE. This predicted (origin) point in the spectrum is marked with an arrow in Fig. 2. While most of the features in the photoelectron spectrum of ZnO^- fit the simulated spectrum rather well, the fit near the arrow is relatively poor. Notice

TABLE I. Results of the Franck–Condon analysis of the photoelectron spectrum of ZnO^- .

	$\omega_e(\text{cm}^{-1})$	$D_0(\text{eV})$	$r_e(\text{\AA})$	$T_0(\text{eV})$
$X^2\Sigma^+(\text{ZnO}^-)$ expt.	625(40)	2.24(5)	1.787(5) ^d	-2.088(10)
$X^2\Sigma^+(\text{ZnO}^-)$ calc. ^a	675	2.20	1.764	-2.03
$X^1\Sigma^+(\text{ZnO})$ expt.	805(40)	1.61(4) ^b	...	0
$X^1\Sigma^+(\text{ZnO})$ calc. ^a	731	1.63	1.719	0
$a^3\Pi(\text{ZnO})$ expt.	...	1.36 ^c	...	0.25
$a^3\Pi(\text{ZnO})$ calc. ^a	573	1.38	1.857	0.26

^aReference 17. (The calculated $a^3\Pi-X^1\Sigma^+$ splitting is T_e not T_0 .)

^bReference 18.

^cUsing $D_0 = 1.61 \text{ eV}$ and $T_0 = 0.25 \text{ eV}$.

^dRelative to the calculated value of 1.719 \AA for $\text{ZnO } X^1\Sigma^+$. $\Delta r_e = +0.07 \text{ \AA}$.

especially the shoulder just to the right (to the low EBE side) of the arrow in the actual spectrum. It is not duplicated in the simulated spectrum. Notice in addition that the vibrational features to the left (to the high EBE side) of the arrow are also fit poorly, not only in height, but in position as well. While these observations are not definitive, they may indicate the presence of weak intensity, photodetachment transitions to the $^3\Pi$ state of ZnO . Based on the possibility that we have indeed observed these transitions, we have tabulated values of T_0 and D_0 for this state in Table I.

DISCUSSION

Among the experimental findings of this work are the inequalities: $D_0(\text{ZnO}^-) > D_0(\text{ZnO})$, $\omega_e(\text{ZnO}^-) < \omega_e(\text{ZnO})$, and $r_e(\text{ZnO}^-) > r_e(\text{ZnO})$. At first glance, the first of these seems inconsistent with the others, since it says that the ZnO^- bond is stronger than the ZnO bond, while the second and third inequalities imply the opposite. Most reasonable electronic structure arguments envision the addition of an extra electron to the lowest energy antibonding orbital of ZnO to form ZnO^- , implying a weaker bond, a smaller vibrational frequency, and a longer bond length for ZnO^- than for ZnO . In light of this, it is the stronger bond in ZnO^- than in ZnO that is the anomaly.

An understanding of these initially perplexing results springs from a detailed examination of the bonding in neutral ZnO . This is provided by Bauschlicher and Partridge¹⁷ in their accompanying theoretical paper on ZnO and ZnO^- . There, they reconcile our seemingly contradictory experimental results, while at the same time confirming them. Consider, as they did, the $^1\Sigma^+$ and the $^3\Pi$ states of neutral ZnO and the separated atom states to which they dissociate. Their work shows that the $^3\Pi$ state dissociates into the ground-state atoms, $\text{Zn}(^1S) + \text{O}(^3P)$, while the $^1\Sigma^+$ state formally dissociates into $\text{Zn}(^1S) + \text{O}(^1D)$, 1.97 eV in energy above the $\text{Zn}(^1S) + \text{O}(^3P)$ asymptote. Even though the $^3\Pi$ state dissociates to its ground-state atoms, however, it is not the ground state of ZnO . Their calculations show that the $^1\Sigma^+$ potential-energy curve dips below the $^3\Pi$ curve in energy, making the $^1\Sigma^+$ state the ground state of ZnO . They explain the depth of the $X^1\Sigma^+$ curve as being due to a strong contribution from the heterolytic $B^1\Sigma^+$ state. This state correlates to the $\text{Zn} + ({}^2S) + \text{O}^- ({}^2P)$ asymptote, located $\sim 6 \text{ eV}$

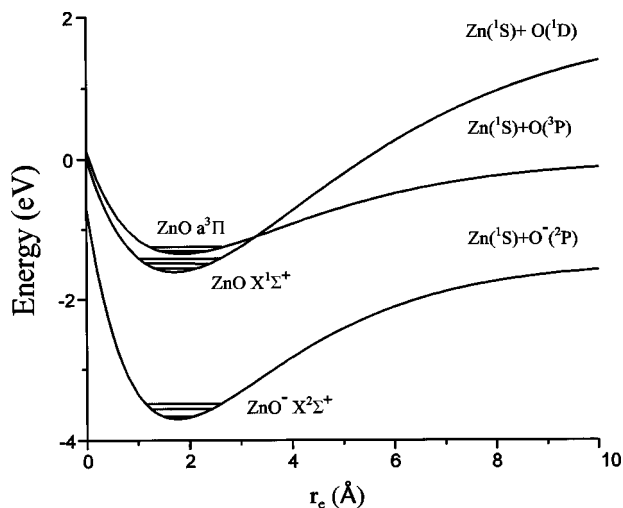


FIG. 3. The potential-energy curves for the $X^1\Sigma^+$ and $a^3\Pi$ states of ZnO along with that for the $X^2\Sigma^+$ state of ZnO^- , all modeled as Morse potentials using parameters from the work of Bauschlicher and Partridge. (Ref. 17)

above the $\text{Zn}(^1S)+\text{O}(^1D)$ asymptote. Figure 3 shows the $X^1\Sigma^+$ and $a^3\Pi$ potential-energy curves for ZnO along with the $X^2\Sigma^+$ curve for ZnO^- , all modeled as Morse potentials using parameters from the work of Bauschlicher and Partridge.¹⁷

The $D_0(\text{ZnO}^-) > D_0(\text{ZnO})$ anomaly can now be rationalized. The value of $D_0(\text{ZnO})$ measured by Armentrout¹⁸ and used by us in Eq. (2) above to compute $D_0(\text{ZnO}^-)$ was, in all likelihood, the dissociation energy of the $X^1\Sigma^+$ state²⁶ of ZnO to the $\text{Zn}(^1S)+\text{O}(^3P)$ asymptote. Referenced to that asymptote, Armentrout's value for $D_0(\text{ZnO})$ remains valid, and thus, so is our value for $D_0(\text{ZnO}^-)$. Referring to Fig. 3, it is now easy to see that the energy required for the $X^1\Sigma^+$ state of ZnO to dissociate into its formal atomic asymptote, $\text{Zn}(^1S)+\text{O}(^1D)$, is indeed larger than the energy required for the $X^2\Sigma^+$ state of ZnO^- to dissociate into its asymptote, $\text{Zn}(^1S)+\text{O}(^2P)$. Thus, when the dissociation energy of the $X^1\Sigma^+$ state of ZnO is computed relative to its formally appropriate $\text{Zn}(^1S)+\text{O}(^1D)$ asymptote, its value is 3.58 eV, as compared to a value of 2.24 eV for the dissociation energy of the $^2\Sigma^+$ state of ZnO^- into $\text{Zn}(^1S)+\text{O}(^2P)$. With these changes in reference asymptotes, the inequality, $D_0(\text{ZnO}^-) > D_0(\text{ZnO})$, is reversed to become $D_0(\text{ZnO}^-) < D_0(\text{ZnO})$, in accord with intuition.

ACKNOWLEDGMENTS

We thank C. W. Bauschlicher and H. Partridge for the valuable theoretical support that they gave this work. We

also thank D. G. Leopold for her assistance in guiding us through the use of the PESCAL program, P. B. Armentrout for a discussion regarding his work with ZnO, and K. A. Gingerich for a conversation about the high-temperature materials literature. This work was supported by the Division of Materials Science, Office of Basic Energy Sciences, U. S. Department of Energy under Grant No. DE-FG02-95ER45538. Acknowledgment is also made to The Donors of The Petroleum Research Fund, administered by The American Chemical Society, for partial support of this research (Grant No. 28452-AC6). In addition, D.W.R. thanks The Research Corporation, which also provided partial support for this research.

- ¹W. Hirschwald, in *Current Topics in Materials Science*, Vol. 6, edited by E. Kaldis (North Holland, Amsterdam, 1980), pp. 109–194.
- ²M. S. Chandrasekharaiah, in *The Characterization of High-Temperature Vapors*, edited by J. L. Margrave (Wiley, New York, 1967), pp. 495–500.
- ³S. Monticone, R. Tufeu, and A. V. Kanaev, *J. Phys. Chem. B* **102**, 2854 (1998).
- ⁴L. Brewer and D. F. Mastick, *J. Chem. Phys.* **19**, 834 (1951).
- ⁵L. Brewer, *Chem. Rev.* **52**, 1 (1953).
- ⁶W. J. Moore and E. L. Williams, *J. Phys. Chem.* **63**, 1516 (1959).
- ⁷W. J. Moore and E. L. Williams, *Discuss. Faraday Soc.* **28**, 86 (1959).
- ⁸E. A. Secco, *Can. J. Chem.* **38**, 596 (1960).
- ⁹T. C. M. Pillay, *J. Electrochem. Soc.* **109**, 76C, Abstract 134 (1962).
- ¹⁰W. Hirschwald, F. Stolze, and I. N. Stranski, *Z. Phys. Chem., Neue Folge* **42**, S, 96 (1964).
- ¹¹D. F. Anthrop and A. W. Searcy, *J. Phys. Chem.* **68**, 2335 (1964).
- ¹²B. G. Wicke, *J. Chem. Phys.* **78**, 6036 (1983).
- ¹³O. Gropen, U. Wahlgren, and L. Pettersson, *Chem. Phys.* **66**, 459 (1982).
- ¹⁴C. W. Bauschlicher and S. R. Langhoff, *Chem. Phys. Lett.* **126**, 163 (1986).
- ¹⁵M. Dolg, U. Wedig, H. Stoll, and H. Preuss, *J. Chem. Phys.* **86**, 2123 (1987).
- ¹⁶E. G. Bakalbassis, M. A.-D. Stiakaki, A. C. Tsipis, C. A. Tsipis, *Chem. Phys.* **205**, 389 (1996).
- ¹⁷C. W. Bauschlicher and H. Partridge, *J. Chem. Phys.* **109**, 8430 (1998), following paper.
- ¹⁸D. E. Clemmer, N. F. Dalleska, and P. B. Armentrout, *J. Chem. Phys.* **95**, 7263 (1991).
- ¹⁹L. R. Watson, T. L. Thiem, R. A. Dressler, R. H. Salter, and E. Murad, *J. Phys. Chem.* **97**, 5577 (1993).
- ²⁰E. S. Prochaska and L. Andrews, *J. Chem. Phys.* **72**, 6782 (1980).
- ²¹J. V. Coe, J. T. Snodgrass, C. B. Freidhoff, K. M. McHugh, and K. H. Bowen, *J. Chem. Phys.* **84**, 618 (1986).
- ²²H. W. Sarkas, J. H. Hendricks, S. T. Arnold, V. L. Slager, and K. H. Bowen, *J. Chem. Phys.* **100**, 3358 (1994).
- ²³P. M. Dehmer and W. A. Chupka, *J. Chem. Phys.* **62**, 4525 (1975).
- ²⁴K. M. Ervin and W. C. Lineberger, in *Advances in Gas Phase Ion Chemistry*, Vol. 1, edited by N. G. Adams and L. M. Babcock (JAI, Greenwich, 1992).
- ²⁵PESCAL Fortran program, written by K. M. Ervin and W. C. Lineberger.
- ²⁶“Because the reaction of $\text{Zn}^+(^2S)+\text{NO}_2(^2A)\rightarrow\text{ZnO}(^1\Sigma^+)+\text{NO}^+(^1\Sigma^+)$ is spin-allowed, formation of the ZnO ground state at the threshold for reaction is expected” (P. B. Armentrout, private communication).